

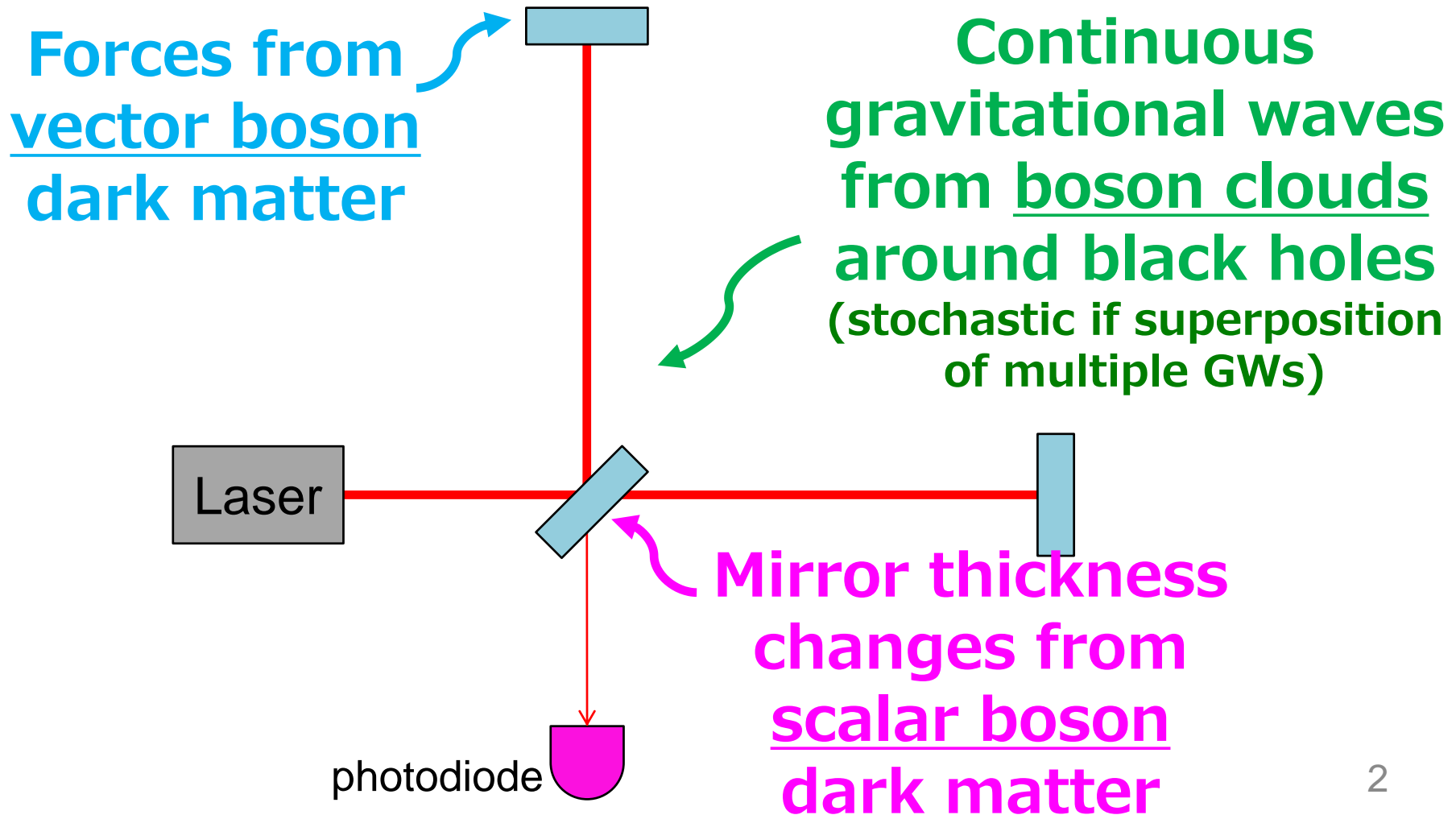
Constraints on **ultralight bosons** using data from gravitational wave detectors

Yuta Michimura

Department of Physics, University of Tokyo

Ultralight Boson

- Can be searched in multiple ways with GW detectors
- See [my last seminar talk](#) for review on ultralight boson dark matter searches



As Dark Matter

- Behaves as classical wave fields rather than particles

$$f = 242 \text{ Hz} \left(\frac{m_b}{10^{-12} \text{ eV}} \right)$$

- Superposition of many waves
→ **stochastic fluctuation** of amplitude and phase

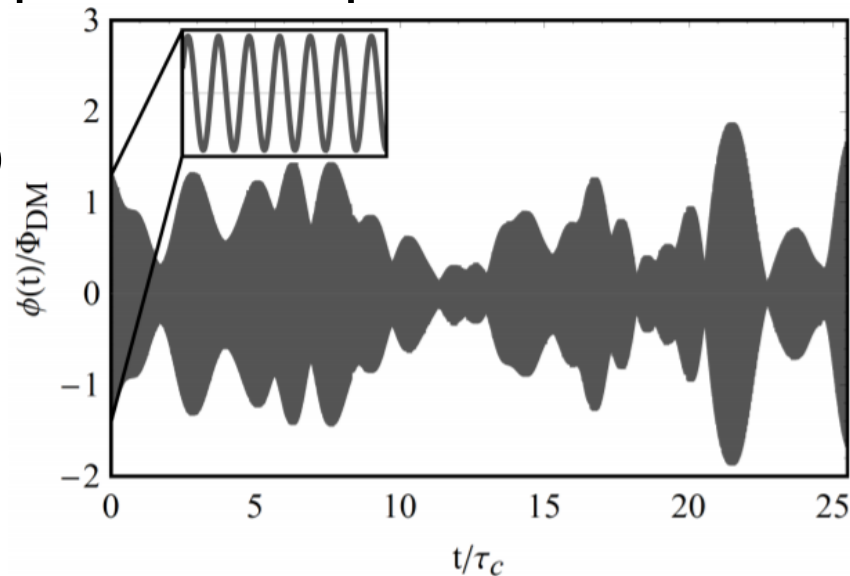
- Coherent time

$$\tau = \frac{2\pi}{m_b v^2}$$

$$Q \sim \frac{\pi}{v^2} \sim 10^6$$

$$\omega = m_b$$

dark matter
velocity ($10^{-3} c$)



- Vector boson field give oscillating force
- Scalar boson field changes optical thickness

G. P. Centers+
[arXiv:1905.13650](https://arxiv.org/abs/1905.13650)

Black Hole Superradiance



- Boson cloud around spinning black hole can be formed through superradiant scattering
 - Boson field amplitude is amplified (upto $\sim 10\%$ of BH mass)
 - Penrose process (extracting energy and spin from Kerr black hole)
 - could explain abundance of low spin BHs

- Boson cloud will emit continuous GWs (frequency equal to **2x** that of boson field)

Purely gravitational search for bosons

$$f_{\text{GW}} \simeq 483 \text{ Hz} \left(\frac{m_b}{10^{-12} \text{ eV}} \right) \left[1 - \frac{6}{25} \left(\frac{M_{\text{BH}}}{10 M_\odot} \frac{m_b}{10^{-12} \text{ eV}} \right) \right]$$

[Phys. Rev. Lett. 123, 171101 \(2019\)](https://arxiv.org/abs/1905.07760)

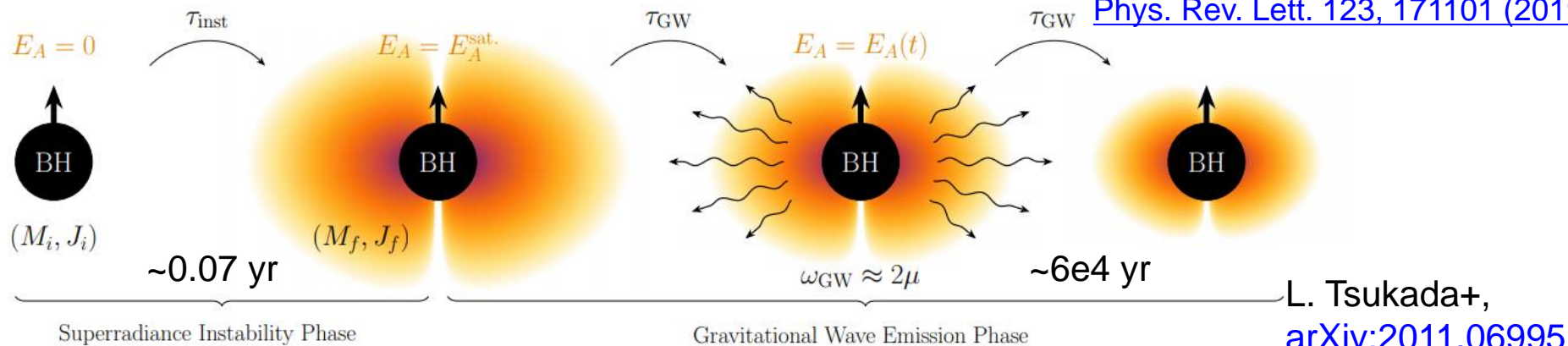


FIG. 1. A schematic representation of the evolution of the superradiance instability and subsequent GW emission. Initial (e.g. quantum) fluctuations in the Proca field seed the instability, leading to an exponentially growing boson cloud around the spinning BH (with growth timescale τ_{inst}). The Proca cloud grows at the expense of BH angular momentum and mass: $M_i - M_f = E_A^{\text{sat.}} > 0$. After saturation, in the GW emission phase the cloud slowly decays with timescale τ_{GW} by emitting monochromatic gravitational radiation at frequency $\omega_{\text{GW}} \approx 2\mu$ (see also Eq. (8)), until the cloud's mass is too small to emit detectable GWs, or an unstable higher azimuthal mode begins dominating the dynamics.

Recent Searches

- H.-K. Guo+, [Communications Physics 2, 155 \(2019\)](#) **Vector** **DM**
Searching for dark photon dark matter in LIGO O1 data
- S. Morisaki+, [arXiv:2011.03589 \(2020\)](#) **Vector** **DM**
Improved sensitivity of interferometric gravitational wave detectors to ultralight vector dark matter from the finite light-traveling time
- S. Vermeulen+, [LIGO-P2100053 \(2021\)](#) **Scalar** **DM**
Upper limits for scalar field dark matter from GEO600
- V. Dergachev & M. A. Papa, [Phys. Rev. Lett. 123, 101101 \(2019\)](#) **Vector** **CW**
Sensitivity Improvements in the Search for Periodic Gravitational Waves Using O1 LIGO Data
- C. Palomba+, [Phys. Rev. Lett. 123, 171101 \(2019\)](#) **Scalar** **CW**
Direct Constraints on the Ultralight Boson Mass from Searches of Continuous Gravitational Waves
- L. Sun, R. Brito, M. Isi, [Phys. Rev. D 101, 063020 \(2020\)](#) **Scalar** **CW**
Search for ultralight bosons in Cygnus X-1 with Advanced LIGO
- L. Tsukada+, [Phys. Rev. D 99, 103015 \(2019\)](#) **Scalar** **Stochastic**
First search for a stochastic gravitational-wave background from ultralight bosons
- L. Tsukada+, [arXiv:2011.06995 \(2020\)](#) **Vector** **Stochastic**
Modeling and searching for a stochastic gravitational-wave background from ultralight vector bosons

Guo+ (2019)

- *Searching for dark photon dark matter in LIGO O1 data*
- **Data:** aLIGO LHO and LLO O1 / 893 hours
 - 1786 of **1800-sec** data from GWSC
- **Target:** $U(1)_B$ vector boson dark matter
- **Excluded from analysis:**
 - electronic lines
 - within ~ 0.056 Hz of lines listed in [PRD 97, 082002 \(2018\)](#)
 - ← O1 and O2 line identification paper
 - ← Extra veto margin to reduce susceptibility to spectral leakage
 - 331.3-331.9 Hz (calibration lines)
 - ← Not optimal
- **Method:** DFT of 1800-sec data (0.00056 Hz bin, 10-2000 Hz band), **single-Fourier-bin cross-correlation** detection static
- **Result:** **10 outliers** (SNR > 5) found but neighboring bins within 0.2 Hz of the signal bin showed elevated noise (SNR > 4)

Guo+ (2019)

- 95% C.L. upper limit
- Exceeds Eöt-Wash limits
- Even better in the future

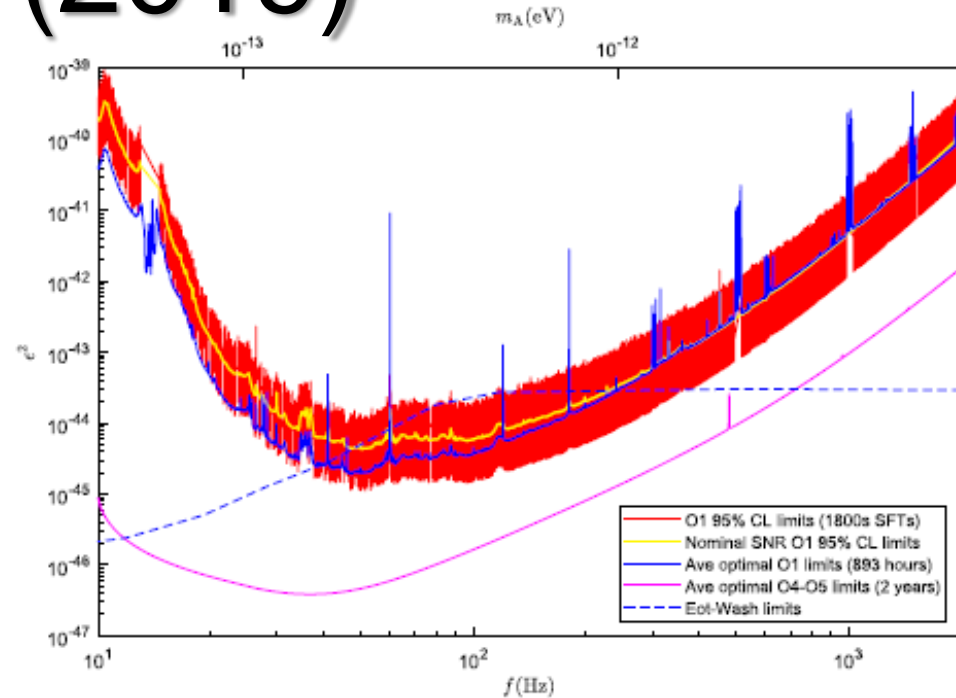


Fig. 4 Derived 95% confidence level upper limits on the coupling parameter ϵ^2 for dark photon-baryon coupling. The broad red band shows the actual upper limits with 1/1800 Hz binning. The yellow curve shows the expected upper limit for an average measured real (SNR) = 0. The dark blue curve shows the “optimal” upper limit expected when the discrete Fourier transform (DFT) binning adjusts with frequency to maintain $\Delta f/f = 10^{-6}$ for the same 893-h observation time. The magenta curve shows the “optimal” upper limit expected for a 2-year, 100%-lifetime run at Advanced LIGO design sensitivity (“O4-O5”). The dashed curve shows upper limits derived from the Eöt-Wash group^{24,25}. This is a fifth-force experiment, whose constraint does not rely on dark photon (DP) being dark matter (DM). The large spikes of red and blue curves, overlaid on top of each other, are induced by known sources of noise, such as vibrations of mirror suspension fibers.



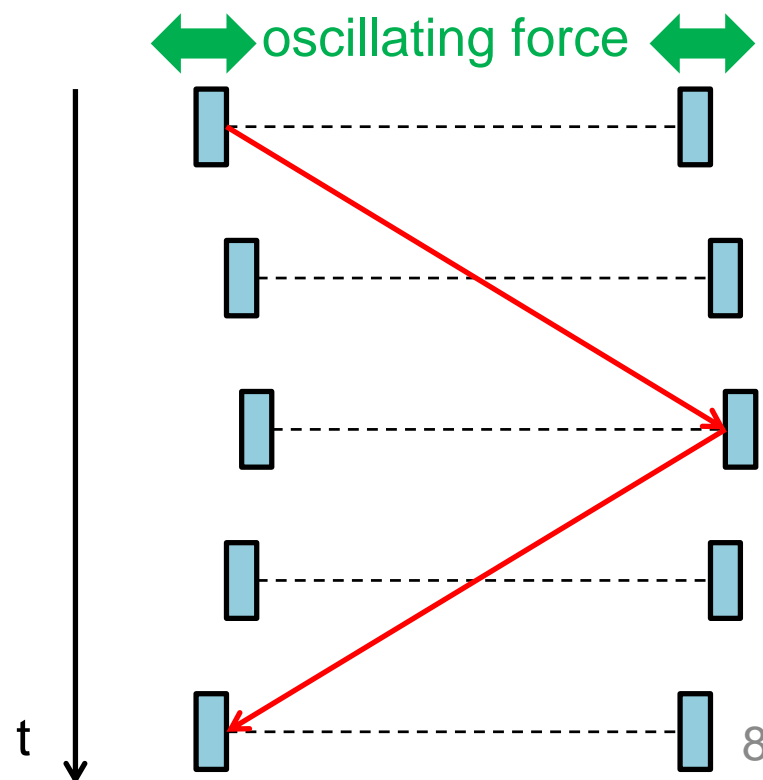
“HIS MASTER’S VOICE”

Morisaki+ (2020)

- *Improved sensitivity of interferometric gravitational wave detectors to ultralight vector dark matter from the finite light-traveling time*
- **Data:** Update of Guo+ (2019) (aLIGO O1 / 893 hours)
- **Target:** $U(1)_B$ and $U(1)_{B-L}$ vector boson dark matter
- Guo+ (2019) didn't take into account of the finite-light traveling time
- Significant when

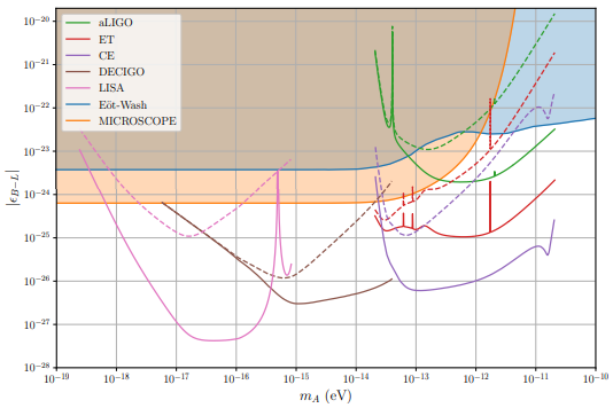
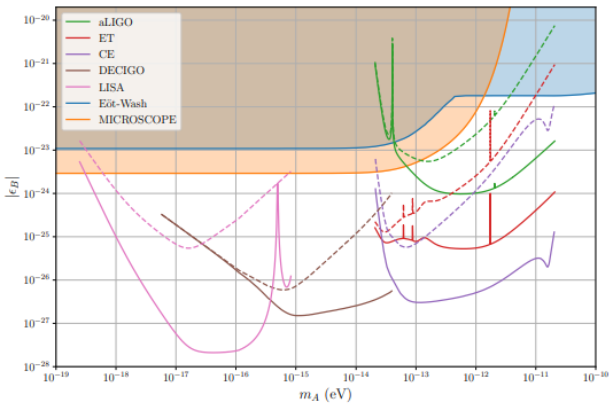
$$m_A \gg vL$$

m_A → boson mass
 v → dark matter velocity ($10^{-3} c$)
 L → arm length



Morisaki+ (2020)

- Updated limit now also exceeds MICROSCOPE limit
- Also calculated limit for B-L



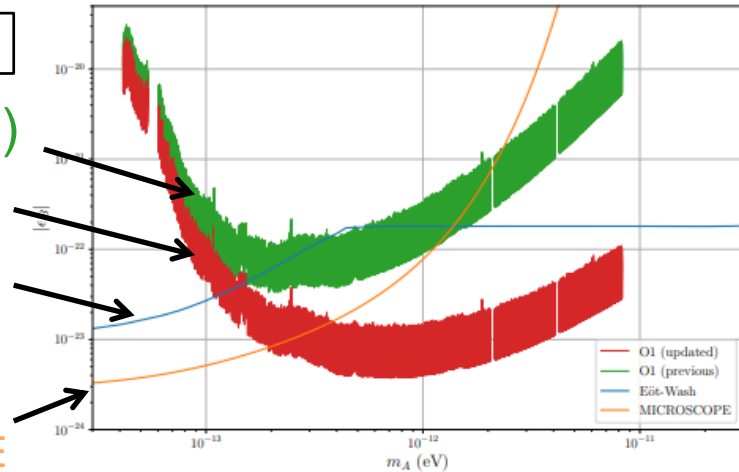
Great sensitivity can be obtained with LISA

B

Guo+ (2019)
updated

Eöt-Wash

MICROSCOPE



B-L

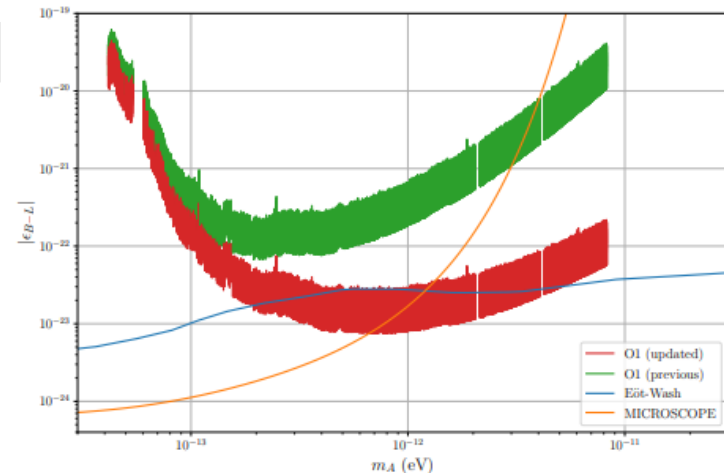


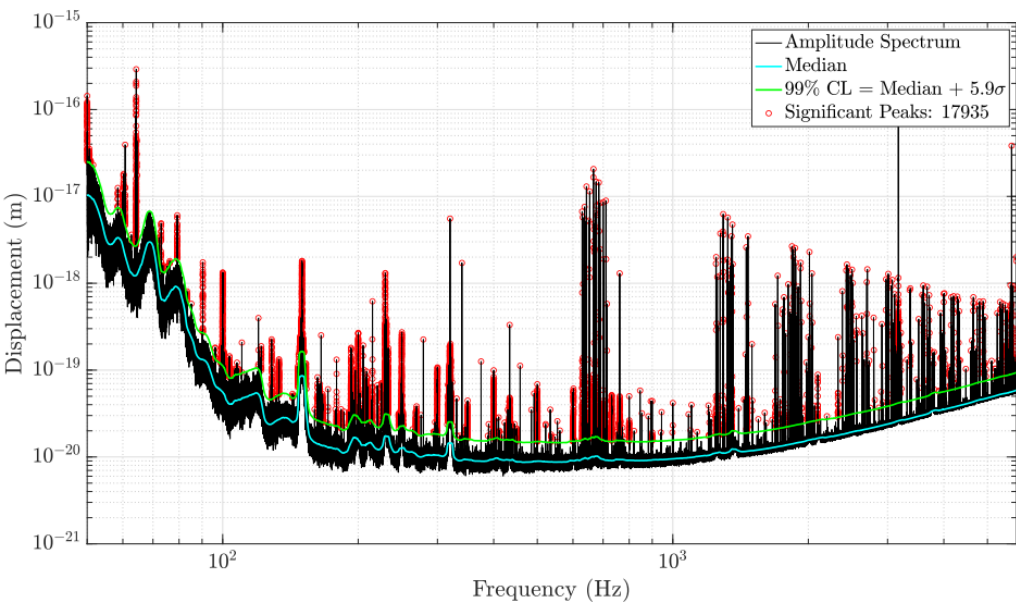
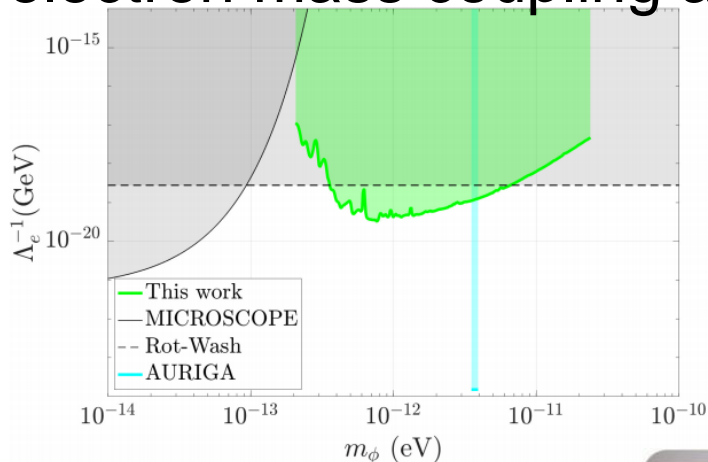
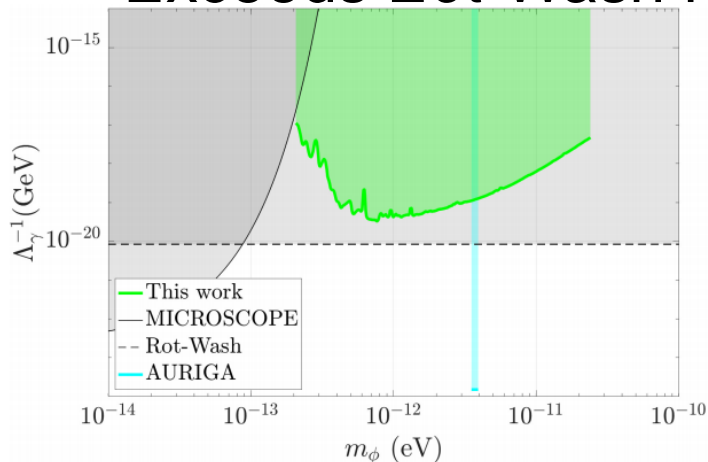
FIG. 3. The constraints given by the LIGO O1, which are updated by the inclusion of the effect from the finite light-traveling time, are shown in red. The green lines represent the constraints previously calculated without the effect. The orange and blue lines represent the constraints from the Equivalence Principle tests. The upper figure is for the $U(1)_B$ case and the lower one is for the $U(1)_{B-L}$ case.

S. Vermeulen+ (2021)

- *Upper limits for scalar field dark matter from GEO600*
- **Data:** GEO600 in 2016 and 2019 / 194 hours
 - 7 of 10^5 sec data
- **Target:** scalar boson that couples to electron mass and fine structure constant
 - **first search** using GW detectors
- **Excluded from analysis:** not discussed coherent time
(optimal DFT)
- **Method:** logarithmic PSD (DFT of τ , 50-6000 Hz band), look-elsewhere effect considered, 10% calibration error included
- **Result:** 17935 peaks above 99% C.L.
 - Rejected if center frequency shift more than 10^{-6}
 - Rejected if the amplitude changed more than 5σ
 - 14 candidates remained
 - 13 candidates had more than x10 higher Q
 - 1 candidate had much longer coherence time

S. Vermeulen+ (2021)

- 99% C.L. upper limit
- Exceeds Eöt-Wash for electron mass coupling at $\sim 10^{-12}$ eV



Dergachev & Papa (2019)

- *Sensitivity Improvements in the Search for Periodic Gravitational Waves Using O1 LIGO Data*
- **Data:** aLIGO O1 data / 4 hours(?) (probably from both LHO and LLO)
- **Target:** continuous GWs (also from vector boson clouds)
- **Excluded from analysis:** not discussed
- **Method:** full-brown all-sky semicoherent search using **Falcon** (fast loosely coherent; last-generation **PowerFlux** search) in 20-200 Hz band
 - sensitivity gain of **30%** compared with previously established PowerFlux
- **Result:** **1111 outliers** found
 - within 0.01 Hz of harmonics of 0.5 Hz (instrumental)
 - hardware-simulated signals (injections)
 - the rest “are close to evident noise disturbances”

Dergachev & Papa (2019)

- List of outliers (full list provided in supplementary)

TABLE II. Outliers that passed detection pipeline excluding outliers within 0.01 Hz from 0.25 Hz comb of instrumental lines. Only the highest SNR outlier is shown for each 0.1-Hz frequency region. Outliers marked with “line” had strong narrow-band disturbances identified near the outlier location. Frequencies are converted to epoch GPS 1130529362.

Index	SNR	Frequency (Hz)	Spin-down (nHz/s)	RA _{J2000} (deg)	DEC _{J2000} (deg)	Description
1	870	52.808 32	0.006	306.634	-83.997	Hardware injection ip5
2	637	191.031 26	-8.652	351.425	-33.552	Hardware injection ip8
4	387	146.169 34	-6.710	359.608	-65.199	Hardware injection ip6
5	376	38.477 93	-6.235	332.323	-14.679	Hardware injection ip12
6	300	108.857 18	-0.006	178.641	-33.400	Hardware injection ip3
22	54	99.976 67	-5.115	100.314	-41.321	Coincident contamination in H1 and L1
23	50	31.512 38	-5.619	226.702	-23.180	Heavy contamination, 0.25 Hz comb in H1, 31.512 Hz line in L1
33	27	65.510 35	-5.419	198.120	-40.763	0.25 Hz comb of instrumental lines
36	23	32.697 85	-9.940	45.757	-37.300	Lack of coherence, contamination in H1
38	21	82.515 84	-3.994	157.388	-46.681	Lack of coherence, 0.25 Hz comb in H1
39	21	81.529 83	-6.310	332.731	-45.648	0.25 Hz comb of instrumental lines
40	21	107.136 43	-6.677	12.094	-57.316	Coincident artifacts at 107.12 Hz in H1 and L1
42	20	113.011 28	1.044	304.688	9.253	0.25 Hz comb of instrumental lines
45	19	90.656 42	-6.944	302.827	59.828	No coherence, disturbed H1 spectrum
46	19	62.806 72	-7.985	276.491	-12.515	Sharp bin-centered line in L1 at 62.8 Hz
47	19	45.018 09	-1.227	186.589	28.604	Lines in H1 and L1 at 45 Hz, contaminated spectrum
48	18	133.307 55	-6.548	124.281	-50.348	Line in L1 at 133.33 Hz
49	18	49.964 16	-9.906	335.191	-18.085	Highly contaminated spectrum
50	18	164.683 48	-4.927	48.010	-9.672	Line in L1 at 164.7 Hz
51	18	86.515 03	-5.252	56.836	-36.012	Coincident lines at 86.5 Hz, 0.25 Hz comb, sloping spectrum in L1
52	18	48.987 73	-4.410	43.189	-22.949	Highly contaminated H1 and L1 spectrum near 49 Hz
53	18	192.831 87	-7.790	248.222	46.044	Contaminated H1 spectrum
56	18	54.121 24	-9.790	225.480	-16.962	Sharp bin-centered line in L1 at 54.1 Hz
57	17	91.714 46	-8.506	128.301	-28.413	Disturbed spectrum in H1 and L1
58	17	53.930 50	-2.956	212.788	-24.064	Disturbed H1 spectrum
59	17	107.660 22	-9.660	24.618	-6.139	Sharp line in L1 at 107.7 Hz

Details of the cause not provided



Dergachev & Papa (2019)

- Most constraining upper limits in GW amplitude in 100-200 Hz band
- Discussed the detection range for signals from vector boson clouds

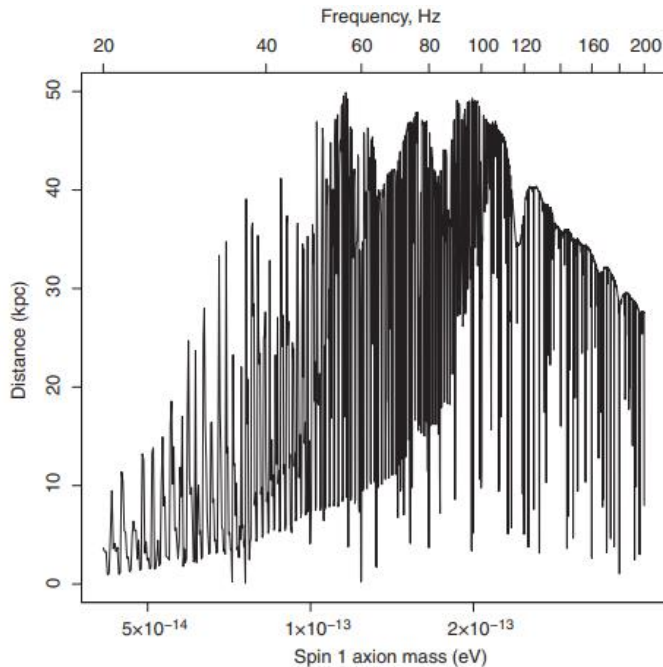


FIG. 3. Sensitivity range to signals from vector boson condensates with parameter $\alpha = 0.03$ around black holes with spin 0.2. This plot was produced using worst-case near-0 spin-down upper limits.

What is α ?
Gravitational
fine structure
constant?

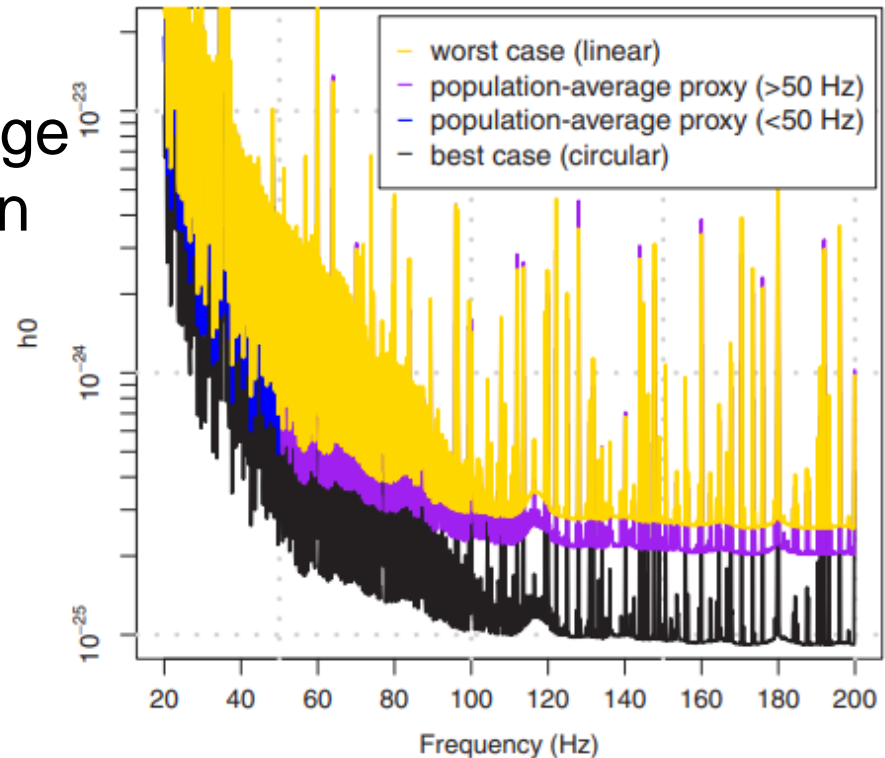


FIG. 1. Upper limits on the intrinsic gravitational wave amplitude at the detectors plotted against signal frequency. The top curve (yellow) shows worst-case upper limits, the next lower curve (purple and blue) the population-average proxy, followed by black curve showing the circular polarization upper limits. The different colors of population-average proxy mark regions with 80% recovery rate (< 50 Hz) and 95% recovery rate (> 50 Hz), as explained in the text.

C. Palomba+ (2019)

- *Direct Constraints on the Ultralight Boson Mass from Searches of Continuous Gravitational Waves*
- **Data:** aLIGO O2 data / 268.37 days
- **Target:** continuous GWs from scalar boson clouds
 - **first time result** from a real search
- **Excluded from analysis:** not discussed
- **Method:** upper limit from all-sky semicoherent search using frequency-Hough pipeline ([Phys. Rev. D 100, 024004 \(2019\)](#)) was **mapped** to boson mass-BH mass plane (with some extended search parameter), 10-2048 Hz band
- **Result:** no outliers discussed in this paper
 - constraints on scalar boson mass
- O2 data is not sensitive enough for signals from ~ 5 Mpc even in most favorable cases

C. Palomba+ (2019)

Exclusion region in boson mass-BH mass plane

Optimistic case

- near (1 kpc)
- high spin
- young age

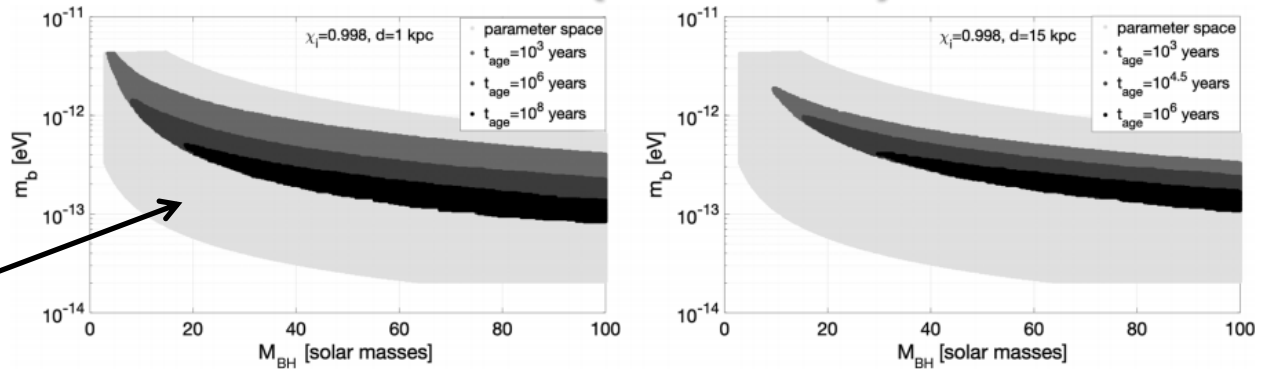


FIG. 2. 95% C.L. exclusion regions in the plane $m_b - M_{\text{BH}}$ assuming a maximum distance $d = 1$ kpc (left plot) and $d = 15$ kpc (right plot), a black hole initial adimensional spin $\chi_i = 0.998$, and three possible values for t_{age} : 10^3 , 10^6 , 10^8 yr (left plot) and 10^3 , $10^{4.5}$, 10^6 yr (right plot). The larger light gray area is the accessible parameter space. As expected, the extension of the excluded region decreases for increasing t_{age} (corresponding to darker color).

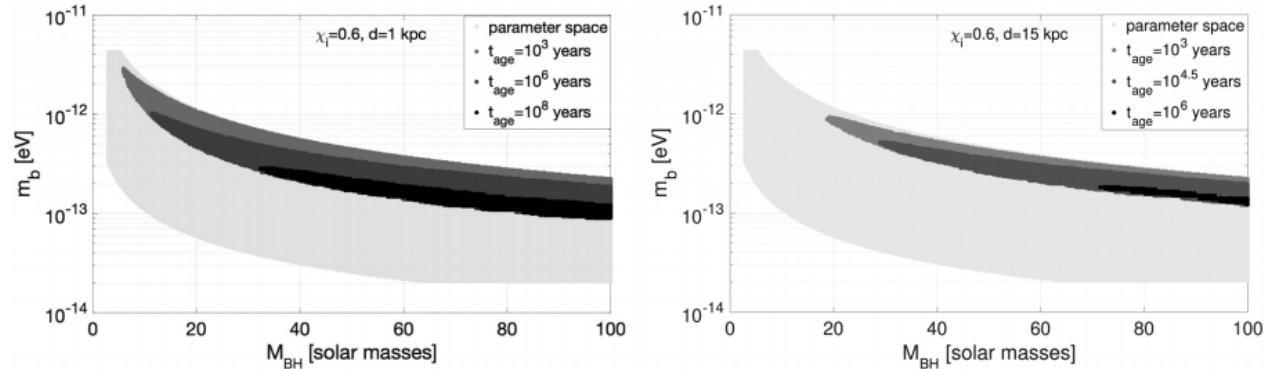


FIG. 3. 95% C.L. exclusion regions in the plane $m_b - M_{\text{BH}}$ assuming a maximum distance $d = 1$ kpc (left plot) and $d = 15$ kpc (right plot), a black hole initial adimensional spin $\chi_i = 0.6$, and three possible values for t_{age} : 10^3 , 10^6 , 10^8 yr (left plot) and 10^3 , $10^{4.5}$, 10^6 yr (right plot). Color code as in previous figure. As expected, the excluded region decreases for increasing t_{age} .

Exclusion depends on

- BH spin
- distance
- time since the beginning of the emission t_{age}

Complementary BH spin measurements by **x-ray** binaries, but **more robust** since isolated BHs are used and do not rely on EM observations

Sun, Brito, Isi (2020)

- *Search for ultralight bosons in Cygnus X-1 with Advanced LIGO*
Erratum: [Phys. Rev. D 102, 089902 \(2020\)](#)
- **Data:** aLIGO LHO and LLO O2 data / 234 days
- **Target:** continuous GWs from scalar bosons in Cyg X-1
- **Excluded from analysis:** not discussed
- **Method:** directed semicoherent search based on **hidden Markov model** tracking scheme combined with a frequency-domain matched filter, Bessel-weighted F -statistic, 250-750 Hz band
- **Result:** **83 candidates** found
 - 64 overlap with known instrumental lines
 - 13 increased significance when analyzing Hanford only
 - 6 had increased significance when searching one half of data→ unable to claim detection

Sun, Brito, Isi (2020)

- **Cygnus X-1 (はくちょう座X-1)**
 - binary of BH and blue supergiant star
 - relatively high BH mass (14.8 Msun)
 - close to Earth (1.86 kpc)
 - large uncertainty in age and spin
(compared with CBC remnants)
 - some measurements indicate BH spin is too high (>0.95) to support boson cloud
 - impact of accretion from the companion is not perfectly understood (assumed that the effect is small here)

TABLE I. Cygnus X-1 parameters.

Parameter	Symbol	Value	Reference
Black hole mass (M_{\odot})	M	14.8 ± 1.0	[54]
Mass ratio	q	1.29 ± 0.15	[55]
Spin	χ	≥ 0.95	[44]
Age (yr)	t_{age}	$[4.8, 7.6] \times 10^6$	[44]
Right ascension	α_*	$19^{\text{h}}58^{\text{m}}22^{\text{s}}$	[56]
Declination	δ_*	$35^{\circ}12'0.6''$	[56]
Inclination (deg)	i	27.1 ± 0.8	[54]
Distance (kpc)	d	1.86 ± 0.12	[55]
Orbital period (days)	P	5.599829 ± 0.000016	[54]
Projected semimajor axis (l-s)	a_0	$25.56^{+3.15}_{-3.11}$	[54]

Sun, Brito, Isi (2020)

- 83 candidates that exceed the threshold (1% false alarm probability) are all vetoed

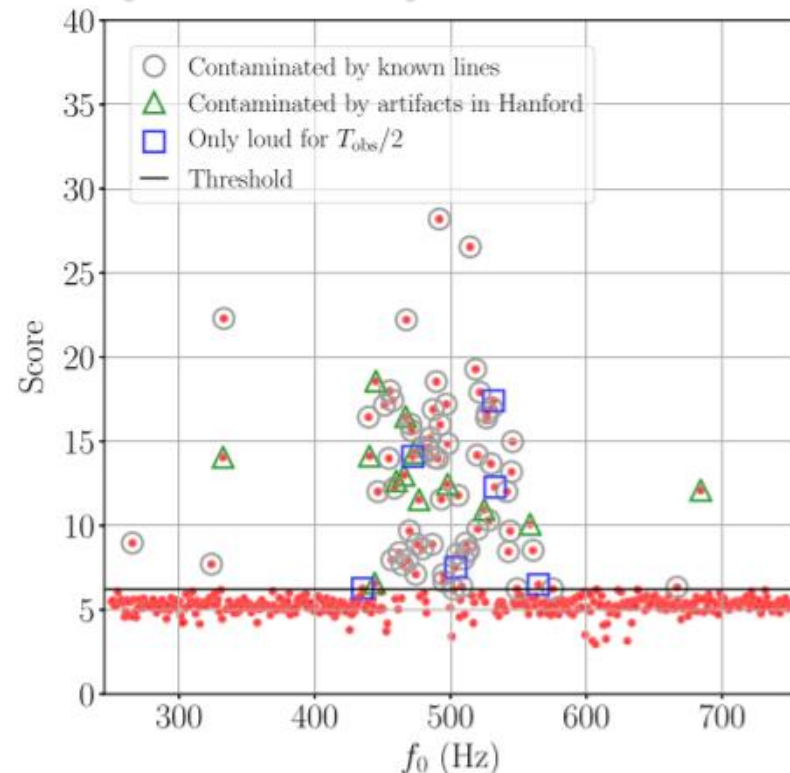


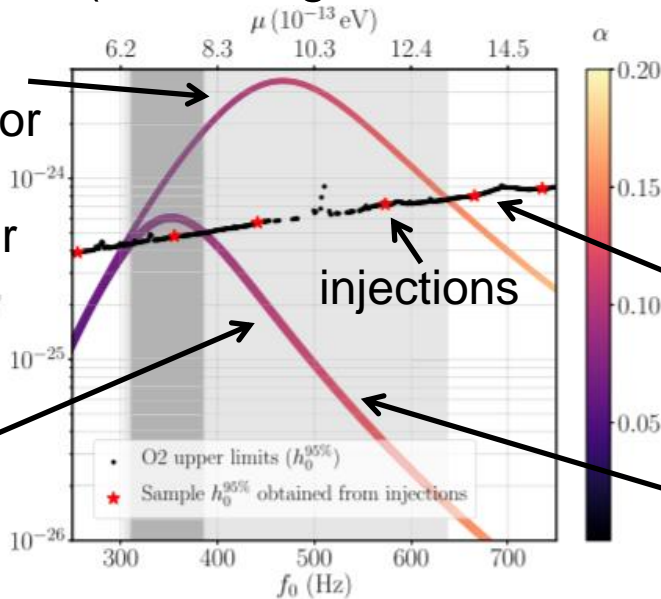
FIG. 1. Detection score S in each 1-Hz sub-band as a function of f_0 . Red dots above the black line (1% false alarm probability threshold $S_{\text{th}} = 6.22$) are the first-pass candidates. Red dots marked by grey circles are vetoed due to contamination by known instrumental lines. Candidates marked by green triangles are vetoed because their scores are increased when analyzing Hanford only rather than the two detectors combined but below threshold when analyzing Livingston only. Candidates marked by blue squares are vetoed because their scores are increased in one half of T_{obs} but below threshold in the other half. No candidate survives all vetoes.

Sun, Brito, Isi (2020)

- Depend on the BH spin and age of Cygnus X-1
- If BH has an age of 5×10^6 year and if it was born with a nearly extremal initial spin (0.99), $5.8 \leq \mu / (10^{-13} \text{ eV}) \leq 8.0$ is disfavored (assuming boson does not self-interact significantly)

Analytically estimated strain for t_{age} of 1×10^5 year (potential younger age of Cyg X-1)

Analytically estimated strain for t_{age} of 5×10^6 year



Erratum: [Phys. Rev. D 102, 089902 \(2020\)](#)

$$\alpha = \frac{GM_{\text{BH}}\mu}{\hbar c^3} \text{ gravitational fine structure constant}$$

strain upper limit

When boson mass is high, h_0 decreases because the time scale of the GW signal τ_{GW} decreases

FIG. 1. Frequentist strain upper limits at 95% confidence ($h_0^{95\%}$) and disfavored scalar boson mass range. The colored curves show the numerically estimated signal strain (h_0) as a function of boson mass (top axis) and GW frequency (bottom axis). The thick and thin curves correspond to $t_{\text{age}} = 5 \times 10^6$ yr and 1×10^5 yr, respectively. The color stands for the fine-structure constant (α). The black dots indicate $h_0^{95\%}$ obtained from the search, assuming the electromagnetically measured orientation $\iota = 27.1^\circ \pm 0.8^\circ$. The red stars mark $h_0^{95\%}$ obtained through injections in O2 data in six sample 1-Hz sub-bands. Sub-bands without a marker were vetoed. The shaded region marks the parameter space where $h_0^{95\%}$ beats the analytically estimated strain, and hence corresponds to the disfavored boson mass range without a detection: $6.4 \leq \mu / (10^{-13} \text{ eV}) \leq 8.0$ for $t_{\text{age}} = 5 \times 10^6$ yr and $6.3 \leq \mu / (10^{-13} \text{ eV}) \leq 13.2$ for $t_{\text{age}} = 1 \times 10^5$ yr. The source parameters adopted in the analytic estimation are $M = 14.8 M_\odot$, $\chi_i = 0.99$, and $d = 1.86$ kpc.

Sun, Brito, Isi (2020)

- When self-interaction in string axiverse scenario is taken into account, $9.6 \leq \mu / (10^{-13} \text{ eV}) \leq 15.5$ is excluded for a decay constant $f_a \sim 10^{15} \text{ GeV}$

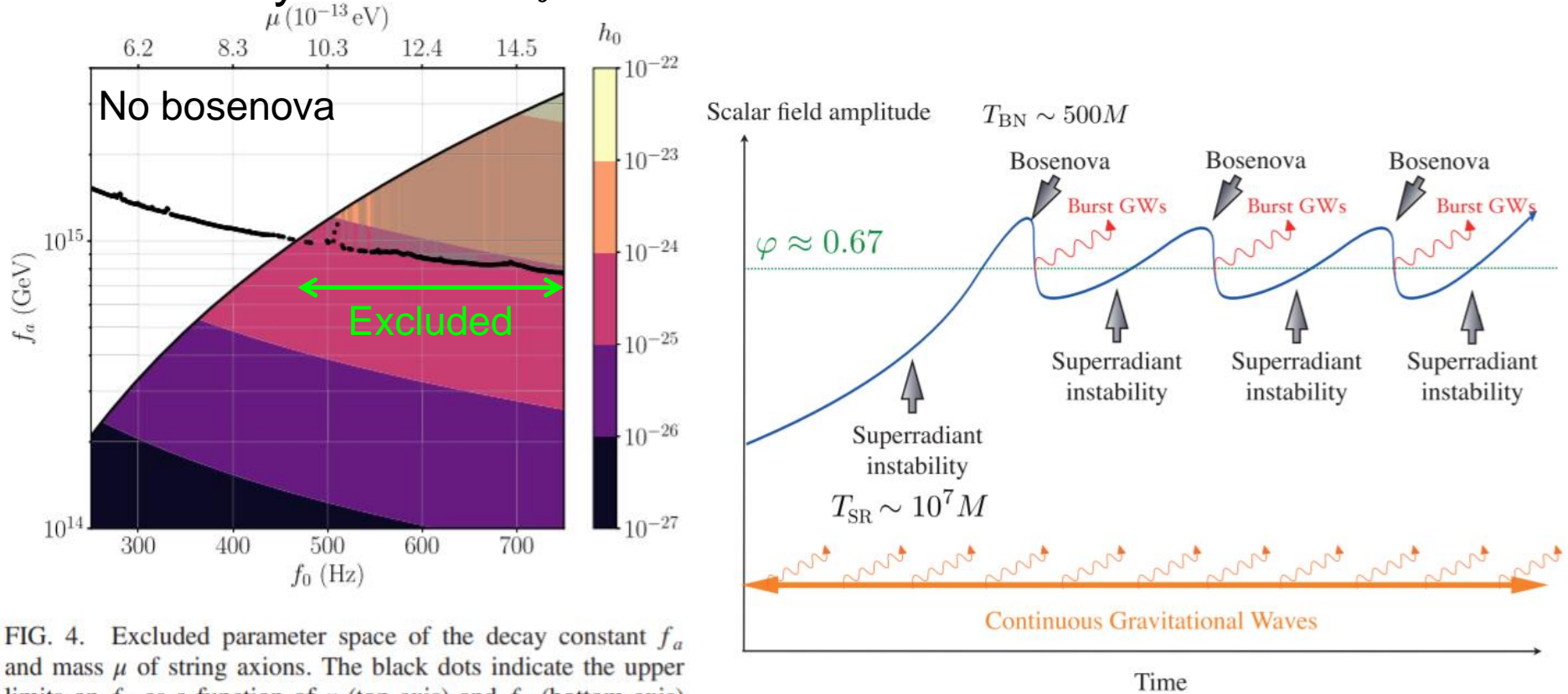


FIG. 4. Excluded parameter space of the decay constant f_a and mass μ of string axions. The black dots indicate the upper limits on f_a as a function of μ (top axis) and f_0 (bottom axis) obtained from the search. The contours indicate the estimated h_0 . The white region is the parameter space where the condition for the bosenova to occur is not satisfied. The shaded region indicates the excluded parameter space.

Yoshino & Kodama,
[PTEP 2015, 061E01, \(2015\)](#)

Tsukada+, (2019)

- *First search for a stochastic gravitational-wave background from ultralight bosons*
- **Data:** aLIGO LHO LLO O1 data
- **Target:** SGWB from scalar boson clouds around isolated BHs and BBH merger remnants
- **Excluded from analysis:** not discussed
- **Method:** Bayesian analysis, cross-correlation
- **Result:** **No statistically significant signal is detected**

→ if BH formation rate is optimistic and spin distribution is optimistic (uniform in $[0,1]$), $2.0 \leq m_b / (10^{-13} \text{ eV}) \leq 3.8$ is excluded at 95% credibility (no limit if less optimistic about spin distribution)

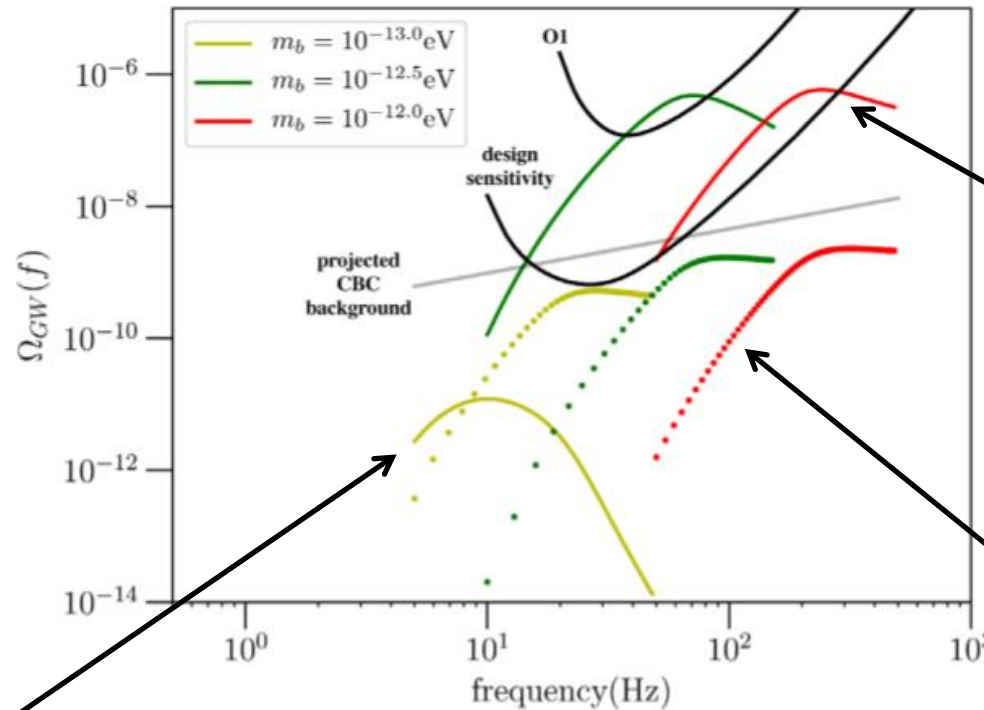
* BH spin distribution is extremely uncertain

Tsukada+, (2019)

Frequency of SGWB cannot be higher than
 $f_{GW} \simeq 483 \text{ Hz} \left(\frac{m_b}{10^{-12} \text{ eV}} \right)$

Low frequency component comes from redshift
 Peaks at the peak of star formation rate ($z=1 \sim 2$)

BH's Schwarzschild radius has to be comparable to boson's Compton wavelength
 ($m_b \sim 10^{-13} \text{ eV}$ for $\sim 10 \text{ Msun}$ BHs)



from isolated BH (assuming uniform spin distribution; optimistic)
 from BBH remnants

FIG. 2. Energy density spectra in the LIGO band overlapped with the power-law integrated curves [36] of LIGO O1 [65] and design sensitivity [66]. Solid curves are spectra based on the isolated BH model with uniform distribution of $\chi \in [0, 1.0]$, whereas dotted curves represent spectra with the BBH merger remnant model. The gray line indicates the projected background of compact binary coalescence (CBC) modeled as a simple power-law spectrum with a power law index of 2/3 [16]. The solid yellow curve is much lower than the other curves, because of the predicted lack of isolated BHs with large enough mass to couple to scalar fields with $m_b = 10^{-13} \text{ eV}$.

Tsukada+, (2019)

- Is it possible to distinguish from CBC background?

Possible inside magenta contour $\ln(\text{Bayes factor}) > 8$

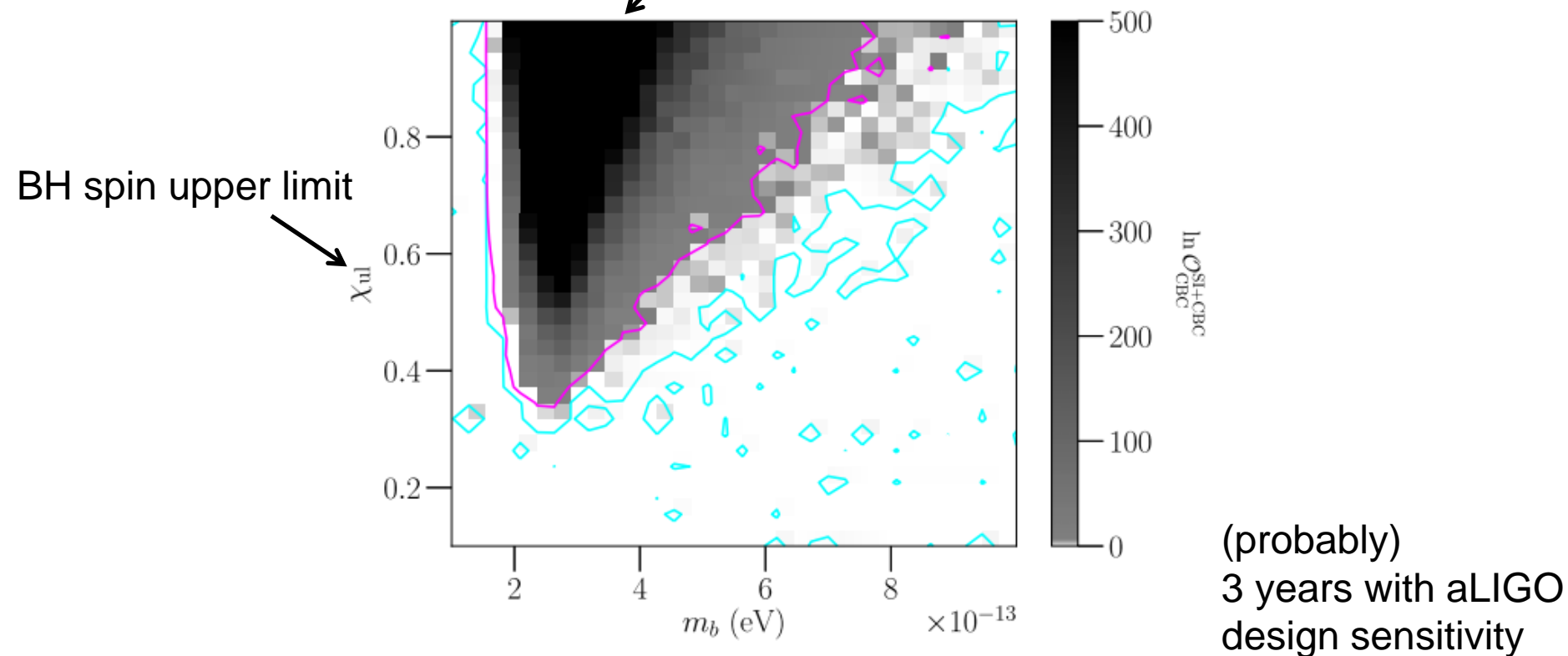


FIG. 6. Gray-scale map of a log Bayes factor between a superradiant instability + CBC model and a CBC-only model. The magenta contour represents $\ln(\text{BF}) = 8$, while the cyan is $\ln(\text{BF}) = 0$.

Tsukada+, (2019)

- Result from O1 data
 - if spin upper limit is varied and lower limit is fixed to 0, no constraint
 - if spin lower limit is varied and upper limit is fixed to 1, $2.0 \leq m_b / (10^{-13} \text{ eV}) \leq 3.8$

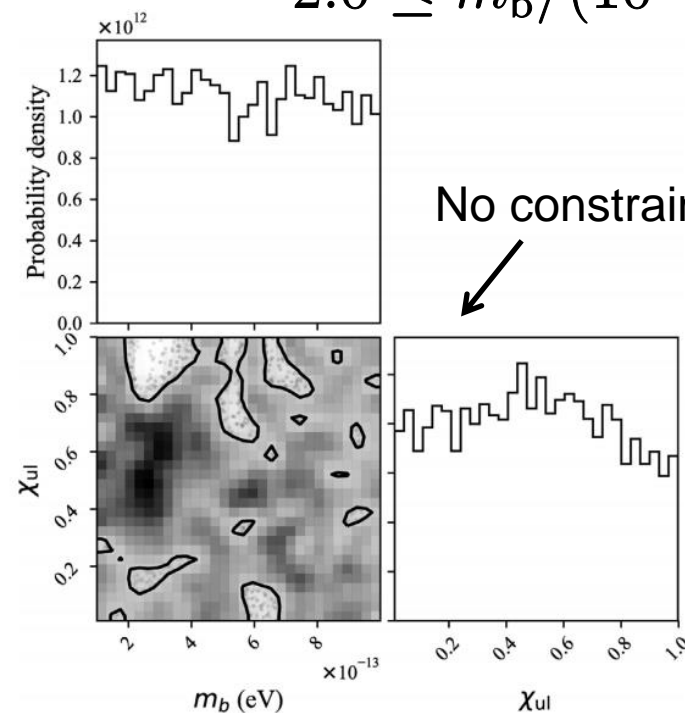


FIG. 7. Posterior results given by the data from the first Advanced LIGO observing run, recovered with the χ_{ul} parametrization. The contour on the two-dimensional posterior represents the 95% confidence level.

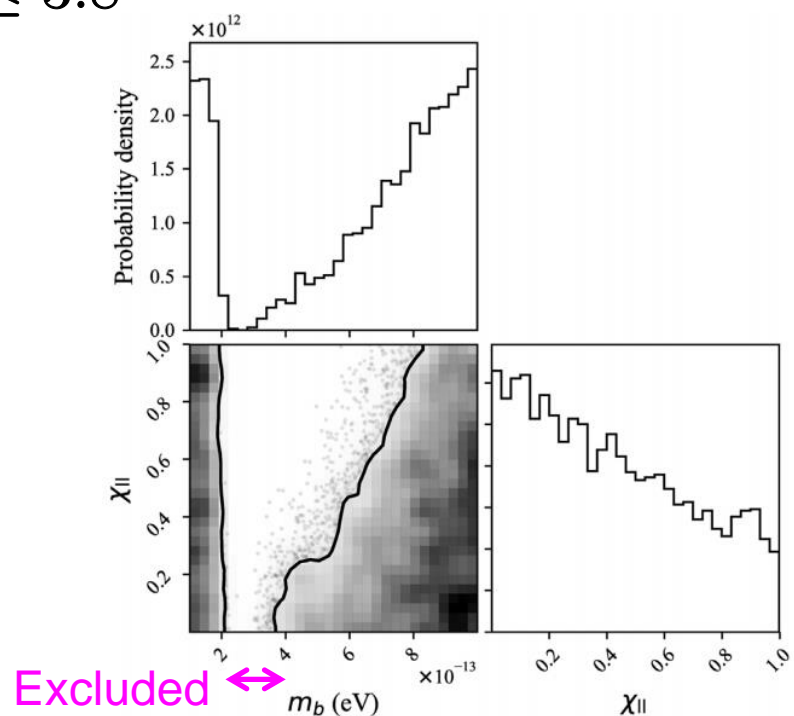


FIG. 8. Posterior results given by the data from the first Advanced LIGO observing run, recovered with the χ_{ll} parametrization. The contour on the two-dimensional posterior represents the 95% confidence level.

Tsukada+, (2020)

- *Modeling and searching for a stochastic gravitational-wave background from ultralight vector bosons*
- **Data:** aLIGO LHO LLO O1 and O2 data
- **Target:** SGWB from **minimally-coupled** (only gravitational, no self-interactions) vector boson clouds around isolated BHs and BBH merger remnants
- **Excluded from analysis:** not discussed
- **Method:** Bayesian analysis, cross-correlation, 20-700 Hz
- **Result:** **No evidence for such signal**

→ if BH formation rate is optimistic and spin distribution is optimistic (uniform in $[0,1]$), $0.8 \leq m_b / (10^{-13} \text{ eV}) \leq 6.0$ is excluded at 95% credibility (narrower but some limit if upper limit of BH spin is larger than ~ 0.2)

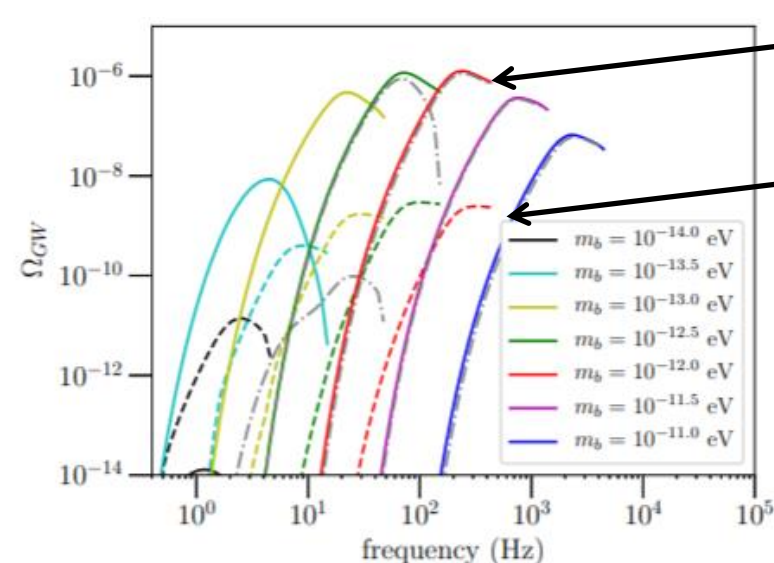
Tsukada+, (2020)

- Vector cloud compared with scalar could
 - significantly stronger GW signal
 - GW power of dominant mode
 - Scalar: scales as $(M_{\text{BH}}m_b)^{14}$
 - Vector: scales as $(M_{\text{BH}}m_b)^{10}$
 - significantly shorter superradiant instability and GW emission timescale

$$(M_{\text{BH}}m_b/\hbar) \sim 0.1$$



Tsukada+, (2019)



from isolated BH (assuming uniform spin distribution; optimistic)

from BBH remnants

Grey dash-dotted lines show scalar case from both channels

FIG. 2. Contribution of different BH formation channels for the total background spectrum Ω_{GW} . Colored solid curves correspond to the spectrum from the isolated BH channel assuming an uniform distribution for the initial BH spin $\chi \in [0, 1]$, whereas colored dashed curves show the spectrum due to the BBH merger remnant channel. For comparison, we also show the total energy spectra that scalar bosons with mass $m_b \geq 10^{-13.5}$ eV would give rise to (gray dashed-dotted lines), including both BH formation channels, and assuming the same BH mass and spin distribution as in the vector case. Note that the spectra for scalar bosons with masses $m_b \leq 10^{-13.5}$ eV do not appear in this figure, because the emission time scale is typically much longer than the BH lifetime in the populations we consider. Note also that the spectra from the BBH merger remnant channel for vector boson masses $m_b \geq 10^{-11.5}$ eV are strongly suppressed because such vector fields tend to induce strong superradiant instabilities only in lighter BHs ($M \lesssim 10 M_\odot$), which are less likely to be produced by the BBH merger remnant channel.

- Dominated by isolated BH channel
- When $m_b > 10^{-12.5}$ eV, GW emission timescale is short and all the energy is emitted within BH lifetime
 - same spectra for scalar and vector
- When $m_b < 10^{-12.5}$ eV GW emission time scale is longer and not all the energy is emitted for scalar case (scalar has longer GW emission timescale)

Tsukada+, (2020)

- Result from O1+O2 data
 - if spin upper limit is varied and lower limit is fixed to 0, some constraint if upper limit is larger than 0.2
 - if spin lower limit is varied and upper limit is fixed to 1, $0.8 \leq m_b / (10^{-13} \text{ eV}) \leq 6.0$

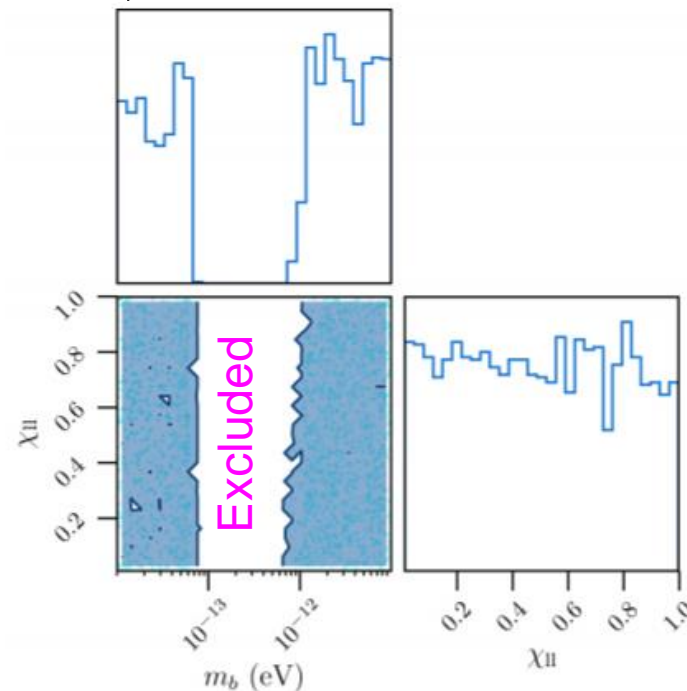
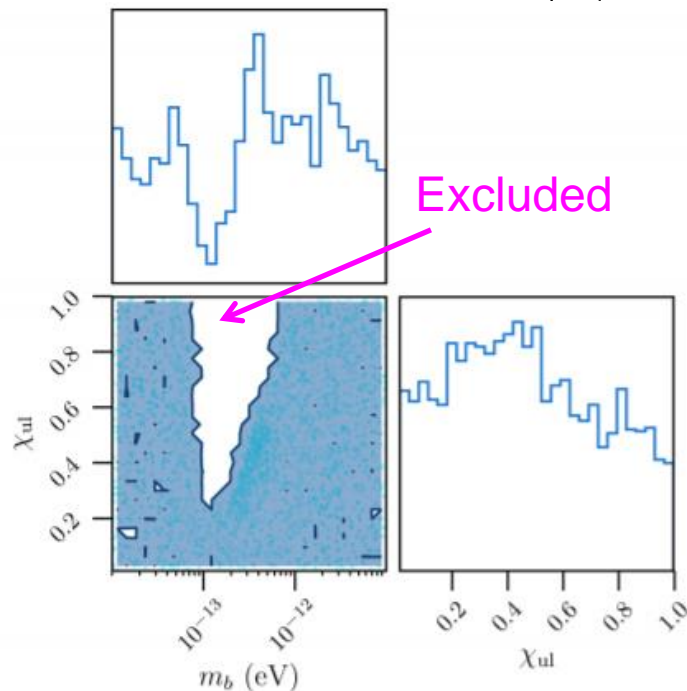


FIG. 7. Posterior results obtained with the data from the first and second observing runs of Advanced LIGO, recovered with the χ_{ul} parameterization. The contour on the two-dimensional posterior represents the 95% confidence level.

FIG. 8. Posterior results, analogous to Fig. 7, for the χ_{II} spin parameterization.

Summary

- Extensive studies of line noises in aLIGO aid data analysis not only for continuous GWs but also for ultralight boson searches
- Having two identical detectors ease our life
- I feel like unknown lines excluded from the analysis could be from something
- Sounds like too many ifs for constraints from GWs from boson clouds, but very interesting
- Injection for validating the data analysis scheme is important



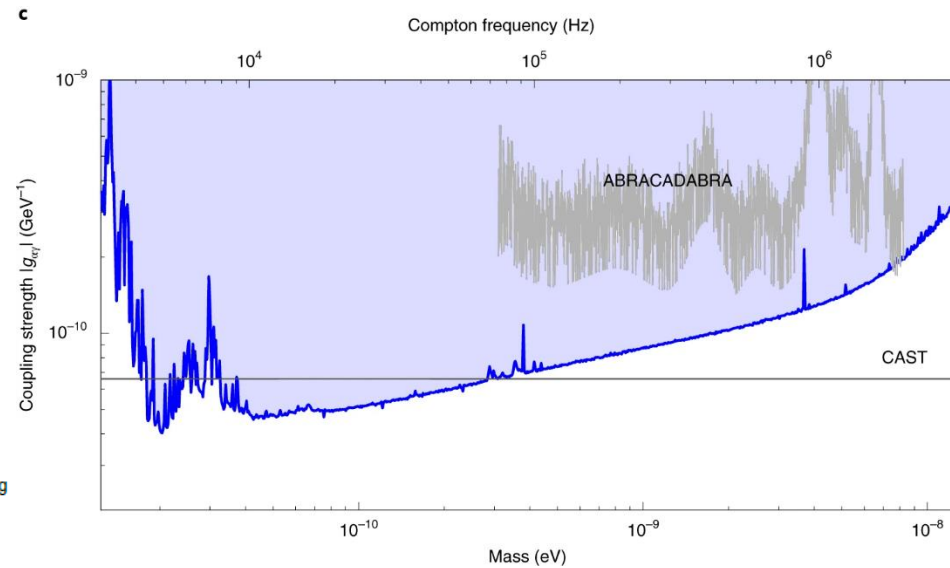
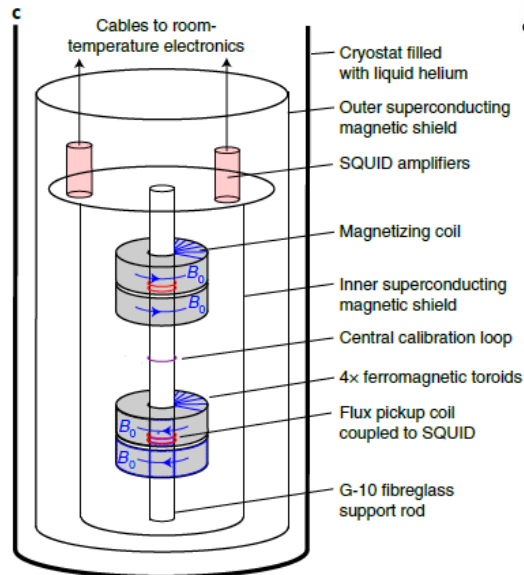
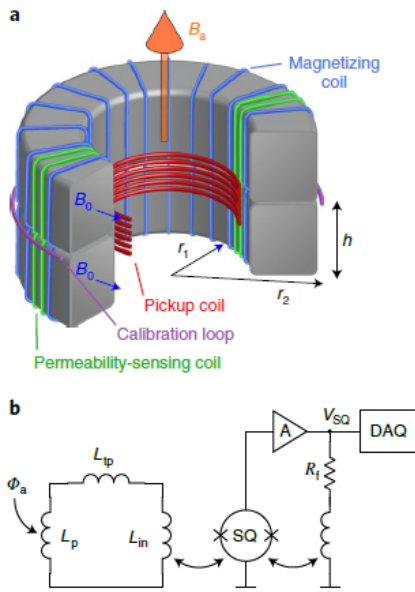
Bonus Slides



Recent Axion Dark Matter Searches

SHAFT (2021)

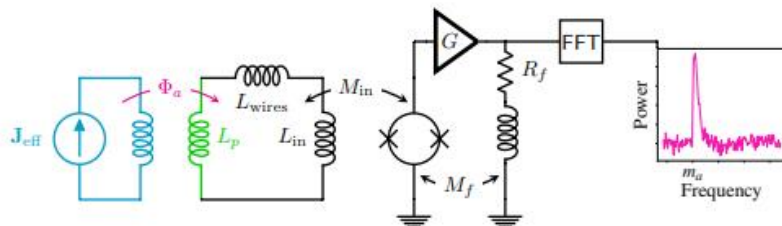
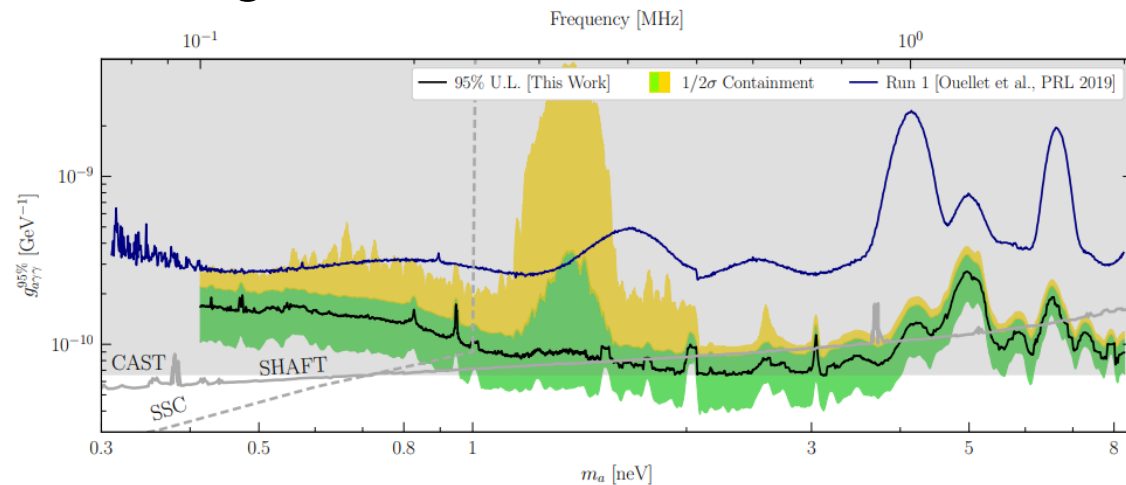
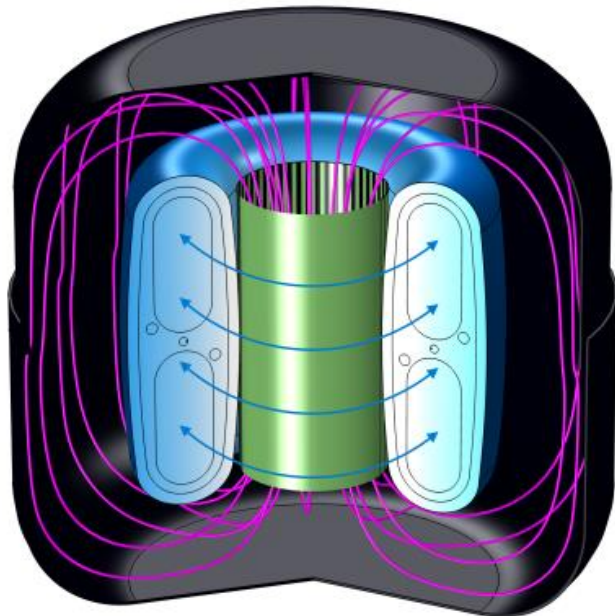
- Search for axion-like dark matter with ferromagnets
- SHAFT: Search for Halo Axions with Ferromagnetic Toroids
- Exceeds CAST limit using 43-hours of data at $\sim 10^{-10}$ eV



Located at Boston University

ABRACADABRA-10 cm (2021)

- *The search for low-mass axion dark matter with ABRACADABRA-10cm*
- Equivalent to CAST limit using 430 hours of data at $\sim 10^{-9}$ eV



Located at MIT in Cambridge, MA

Revisiting DeRocco & Hook (2018)

[Phys. Rev. D 98, 035021 \(2018\)](#)

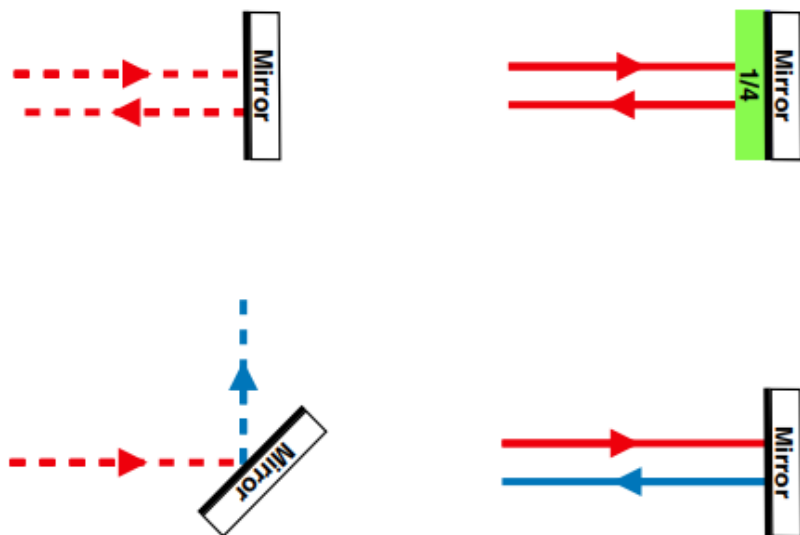


FIG. 1. How to map reflections off of mirrors between axion interferometers and their equivalent gravity wave interferometers. On the left are the gravity wave interferometer set-ups (dashed lines) and on the right are the axion interferometer set-ups (solid lines). Red lines indicate light going in the x direction or \ominus polarized light and blue lines indicate light going in the y direction or \oplus polarized light. The comparison is drawn between the x/y direction of light for GWs and left/right circular polarizations for axion DM because the effect of a GW is a change in the path length between the x and y directions while the effect of axion DM is a change in the path length between right and left circular polarizations.

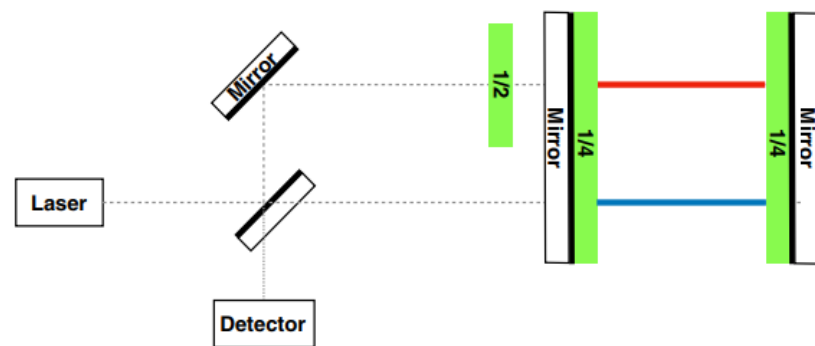
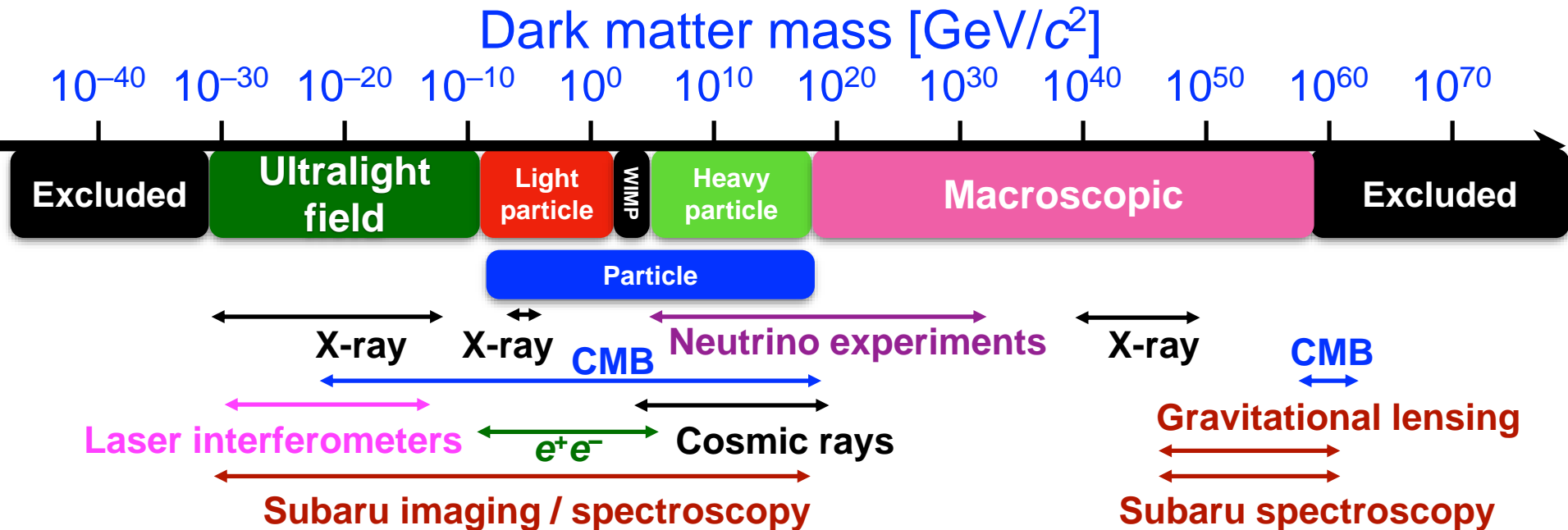


FIG. 3. A diagram of our proposed axion interferometer where the same mirrors are used to form both cavities. The dotted line is linearly polarized light, the red line is \ominus polarized light and the blue line is \oplus polarized light. Two quarter wave plates and a half wave plate are used to maintain the circular polarization of the light. This setup cancels the radiation pressure noise associated with the displacement of the mirror, leaving only noise due to radiation torque. Torque noise in this setup can be several orders of magnitude smaller than the radiation pressure noise experienced by the setup in Fig. 2.

Additional Slides

Ultralight Dark Matter

- Ultralight DM ($< \sim 1$ eV) behaves as classical wave fields
- $$f = 2.4 \text{ Hz} \left(\frac{m_{\text{DM}}}{10^{-14} \text{ eV}} \right)$$
- Laser interferometers are sensitive to tiny length changes from such oscillations



Freq-Mass-Coherence Time

Frequency	Mass	Coherent Time	Coherent Length
0.1 Hz	4.1e-16 eV	0.32 year	3e12 m
1 Hz	4.1e-15 eV	1e6 sec 12 days	3e11 m
10 Hz	4.1e-14 eV	1.2 days	3e10 m
100 Hz	4.1e-13 eV	2.8 hours	3e9 m
1000 Hz	4.1e-12 eV	17 minutes	3e8 m
10000 Hz	4.1e-11 eV	1.7 minutes	3e7 m